A new immersed finite element method for two phase Stokes problems having discontinuous pressure

Gwanghyun Jo[a], Do Y. Kwak[b,*]

[a]*Department of Mathematics, Kunsan National University, Gunsan-si, Jeollabuk-do, Republic of Korea*
[b]*Department of mathematical Sciences, Korea Advanced Institute of Science and Technology, 291 Daehak-ro, Daejeon, Republic of Korea 34141*

Abstract

In this paper, we develop a new immersed finite element method (IFEM) for two phase incompressible Stokes flows. We allow the interface to cut the finite elements. On the non-interface element, standard Crouzeix-Raviart element and P_0 element pair is used. On the interface element, the basis functions developed for scalar interface problems (Kwak et al. *An analysis of a broken P_1-nonconforming finite element method for interface problems, SIAM J. Numer. Anal. (2010)*) are modified in such a way that the coupling between the velocity and pressure variable is different. There are two kinds of basis functions. The first kind of basis satisfies the Laplace-Young condition under the assumption of the continuity of the pressure variable. In the second kind, the velocity is of bubble type and is coupled with the discontinuous pressure, still satisfying the Laplace-Young condition. We remark that in the second kind the pressure variable has two degrees of freedom on each interface element. Therefore, our methods can handle the discontinuous pressure case. Numerical results including the case of the discontinuous pressure variable are provided. We see optimal convergence orders for all examples.

Keywords: immersed finite element method, Crouzeix-Raviart finite element, Two phase Stokes problems, Laplace-Young condition

1. Introduction

Recently, there have emerged many unfitted grid methods to solve interface problems involving interface between two materials. Extended finite element method (XFEM) [26, 4, 27, 5, 21, 8, 29] is one of the popular methods to solve for interface/crack problems based on uniform grids. Some additional basis functions constructed by truncating the shape function along the interfaces are added to the trial/test spaces. Thus, the number of degrees of freedom increase near the interface. For Stokes interface problems, Gross and Reusken proposed a method that adopt an XFEM enrichment of the pressure space, incorporating functions that are discontinuous at the interface in [9, 10, 28].

Meanwhile, Hansbo et al. introduced a so called cut-FEM, combining XFEM and Nitche's method for elliptic interface problems [11, 3]. For Stokes interface problem, iso P_2-P_1 element based cut-FEM type method was proposed [12] where ghost penalty stabilization is used near the interface to avoid instabilities. Also, Wang et al. introduced P_1-nonconforming based cut-FEM method for Stokes interface problems [31], where stabilization terms defined on the transmission edges are used to ensure stability condition. However, all of the methods mentioned above require additional degrees of freedom than the nodal basis functions.

*Corresponding Author. email:kdy@kaist.ac.kr

On the other hand, Z. Li et al. [22, 23] introduced immersed finite element method (IFEM) for elliptic problems, where the basis functions are modified to satisfy the flux type continuity conditions along the interface. The advantage of this scheme is that it does not require additional basis functions. Since then, the error estimates for IFEMs were developed for various elliptic interface problems, see [25, 6, 18, 13] and references therein. The Crouzeix-Raviart P_1-nonconforming based IFEM [18] were used to solve elasticity interface problems in [19]. Also, IFEMs have been applied to various problems, including plasma particle simulation, electric field simulation in composite materials, electroencephalography, fluid-structure interaction, multiphase flows in porous media, elasticity, and Poisson-Boltzmann equation [24, 17, 32, 30, 15, 14, 20].

For Stokes equations, Adjerid et al. [1, 2] introduced immersed discontinuous finite element method, which uses modified Q_1/Q_0 basis functions in the frame work of discontinuous Galerkin methods. The velocity and pressure variables are modified on the interface element so that the basis functions satisfy Laplace-Young condition (see details in [1, 2]). An IFEM based on P_1/Q_1 nonconforming elements are introduced in [16], where modification process is similar to [1, 2]. We remark that the pressure variable in the immersed finite element (IFE) space of [1, 2] or [16] uses the average (on each element) as degrees of freedom on the interface element. Clearly, these elements cannot approximate the pressure variable in general.

In this paper, we develop a new P_1-nonconforming based IFEM for Stokes interface problems where modification of basis functions are different from that in [1] or [16]. On the interface element, we construct two kinds of basis functions for the velocity variables. First kind is related to the continuous pressure. Second kind is of bubble type in the sense that velocity variables has vanishing averages on the edges, and it satisfies Laplace-Young condition for discontinuous pressure. In this way, we construct velocity basis on interface element which is less coupled to pressure basis compared with [1] or [16]. Another aspects of our IFE space is that the pressure basis has two degrees of freedom on the interface element so that it can handle the discontinuity of pressure variable. For the bilinear form, we add stabilization terms across edges as in [12, 19] to make the system stable. The numerical examples including the case of the discontinuous pressure variable are provided. We see optimal convergence rates for both the pressure and velocity variables.

The rest of the paper is organized as follows. We describe an incompressible Stokes interface problem in Section 2 and develop IFEM for the Stokes problems in Section 3. Numerical experiments are reported in Section 4 and the conclusion follows in Section 5.

2. A model problem

Let Ω be a connected polygonal domain in $\mathbb{R}^2$ which is divided into two subdomains Ω^+ and Ω^- by a C^2 interface $\Gamma = \partial\Omega^+ \cap \partial\Omega^-$ (see Figure 1). We assume that subdomains are filled with two incompressible fluids of different viscosities.

The equation describing the steady-state of such fluids is given by

$$
\begin{aligned}
-\operatorname{div}\boldsymbol{\sigma} &= \mathbf{f} && \text{in } \Omega^+ \cup \Omega^-, && (2.1a)\\
\boldsymbol{\sigma}(\mathbf{u}, p) &= 2\mu\boldsymbol{\epsilon}(\mathbf{u}) - p\mathbf{I} && \text{in } \Omega^+ \cup \Omega^-, && (2.1b)\\
\operatorname{div}\mathbf{u} &= 0 && \text{in } \Omega^+ \cup \Omega^-, && (2.1c)\\
\mathbf{u} &= \mathbf{g} && \text{on } \partial\Omega && (2.1d)
\end{aligned}
$$

with the interface conditions

$$
\begin{aligned}
[\![\mathbf{u}]\!]_\Gamma &= 0 \quad \text{on } \Gamma, && (2.2a)\\
[\![\boldsymbol{\sigma}(\mathbf{u}, p)\cdot\mathbf{n}]\!]_\Gamma &= 0 \quad \text{on } \Gamma, && (2.2b)
\end{aligned}
$$

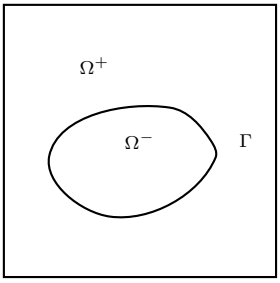

Figure 1: A domain Ω with an interface Γ.

where $\boldsymbol{\epsilon}(\mathbf{u}) = \frac{1}{2}(\nabla\mathbf{u} + \nabla\mathbf{u}^T)$ is the strain tensor, the vector $\mathbf{f}$ is a body force, $\mu > 0$ is a piecewise constant function of the viscosity:

$$\mu = \begin{cases} \mu^+ & \text{in } \Omega^+ \\ \mu^- & \text{in } \Omega^-, \end{cases}$$

and $\mathbf{n}$ is the outward unit normal vector to Γ. For the simplicity, we may assume $\mathbf{g} = 0$. The bracket $[\![\cdot]\!]_\Gamma$ means the jump across the interface

$$[\![\mathbf{u}]\!]_\Gamma := \mathbf{u}|_{\Omega^-} - \mathbf{u}|_{\Omega^+}.$$

We use standard Sobolev space notations (see section 4). Multiplying $\mathbf{v} \in H_0^1(\Omega)^2$ to the left hand side of the equation (2.1a), we get by Green's formula

$$\begin{aligned} & \sum_{s=+,-} \left(-2\mu \int_{\Omega^s} \sum_{i,j} \frac{\partial \epsilon_{ij}(\mathbf{u})}{\partial x_j} v_i + \int_{\Omega^s} \sum_i \frac{\partial p}{\partial x_i} v_i \right) \\ = & \sum_{s=+,-} \int_{\Omega^s} \left(2\mu\boldsymbol{\epsilon}(\mathbf{u}) : \boldsymbol{\epsilon}(\mathbf{v}) - \int_{\Omega^s} p \operatorname{div} \mathbf{v} \right) dx + \sum_{s=+,-} \left(\int_{\partial\Omega^s} (p\mathbf{n} - 2\mu\boldsymbol{\epsilon}(\mathbf{u})\mathbf{n}) \cdot \mathbf{v} \right). \end{aligned} \tag{2.3}$$

Using the jump conditions (2.2a) and (2.2b), we obtain the following variational formulation of problem (2.1a) and (2.1c) : Find the velocity $\mathbf{u} \in (H_0^1(\Omega))^2$ and the pressure $p \in L_0^2(\Omega)$ satisfying

$$a(\mathbf{u}, \mathbf{v}) - b(\mathbf{v}, p) = (\mathbf{f}, \mathbf{v}), \quad \forall \mathbf{v} \in H_0^1(\Omega)^2, \tag{2.4a}$$

$$b(\mathbf{u}, q) = 0, \qquad \forall q \in L_0^2(\Omega), \tag{2.4b}$$

where

$$\begin{aligned} a(\mathbf{u}, \mathbf{v}) &:= \sum_{s=+,-} \int_{\Omega^s} 2\mu\boldsymbol{\epsilon}(\mathbf{u}) : \boldsymbol{\epsilon}(\mathbf{v}) dx \\ b(\mathbf{u}, p) &:= \sum_{s=+,-} \int_{\Omega^s} p \operatorname{div} \mathbf{u}\, dx. \end{aligned}$$

3. An IFEM based on Crouzeix-Raviart element

Let $\{\mathcal{T}_h\}$ be a any structured triangulations of Ω by the triangles of maximum diameter h. We allow the grid to be cut by the interface. We call an element $T \in \mathcal{T}_h$ an *interface element* if the

interface Γ passes through the interior of T, otherwise we call it a *noninterface* element. Let $\mathcal{T}_h^I$ be the collection of all interface elements.

Let the collection of all the edges of $T \in \mathcal{T}_h$ be denoted by $\mathcal{E}_h$. We denote the set of edges cut by the interface Γ by $\mathcal{E}_h^I$, its complement is denoted by $\mathcal{E}_h^N$. Even though the interface Γ is a curve in general, we replace for the simplicity of presentation, the part of interface in T by the line segment connecting the intersection points with ∂T. Therefore, the interface Γ is assumed to be polygonal for the rest of the paper.

3.1. Construction of IFEM basis for Stokes interface problem

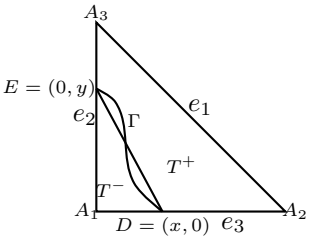

Figure 2: A typical interface triangle

For the noninterface elements, we use classical Crouzeix-Raviart element [7] for the velocity variable which consists of piecewise linear polynomials whose degrees of freedom are the average value along each edge. In other words, for $T \in \mathcal{T}_h \backslash \mathcal{T}_h^I$, let $\mathbf{N}_h(T)$ denote the linear space spanned by the six Lagrange basis functions, $\boldsymbol{\phi}_i = (\phi_{i1}, \phi_{i2})^T,\ i = 1, \cdots, 6$;

$$\mathbf{N}_h(T) = span\{\boldsymbol{\phi}_i \in (P_1)^2 : \frac{1}{|e_j|}\int_{e_j} \phi_{i1} = \delta_{ij},\ j = 1,2,3,\ \frac{1}{|e_j|}\int_{e_j} \phi_{i2} = \delta_{i-3,j},\ j = 4,5,6\}. \quad (3.1)$$

We define the pressure space $M_h(T) \equiv P_0(T)$ to be the space of constant on T.

Now, we consider the interface elements. We adopt the broken P_1-nonconforming finite element introduced in [18, 19] for the velocity. For the pressure we use two pieces of piecewise constant function for the interface element. An important property of the IFEM basis is that it should satisfy the Laplace-Young condition (2.2b) at least weakly. For that purpose, we shall construct two kinds of basis functions: The first kind is unrelated to the pressure; the second kind is coupled with pressure. We assume the three vertices are given by $A_1 = (0,1)$, $A_2 = (0,0)$, $A_3 = (1,0)$ (see Figure 2). For any interface element $T \in \mathcal{T}_h^I$ in general position, all the constructions to be presented below carries over through affine equivalence. Let $\overline{DE}$ be the line segment connecting the intersections of the interface and the edges of a triangle T. This line segment divides T into two parts T^+ and T^-.

We describe the first type. We set, for $i = 1, 2, \cdots, 6$,

$$\boldsymbol{\phi}_i(x,y) = \begin{cases} \boldsymbol{\phi}_i^+(x,y) = \begin{pmatrix} \phi_{i1}^+ \\ \phi_{i2}^+ \end{pmatrix} = \begin{pmatrix} a_1^+ + b_1^+ x + c_1^+ y \\ a_2^+ + b_2^+ x + c_2^+ y \end{pmatrix}, & (x,y) \in T^+, \\ \\ \boldsymbol{\phi}_i^-(x,y) = \begin{pmatrix} \phi_{i1}^- \\ \phi_{i2}^- \end{pmatrix} = \begin{pmatrix} a_1^- + b_1^- x + c_1^- y \\ a_2^- + b_2^- x + c_2^- y \end{pmatrix}, & (x,y) \in T^-, \end{cases} \quad (3.2)$$

and require these functions satisfy the 6 degrees of freedom (3.1), continuity condition (2.2a), and the Laplace-Young condition with zero pressure along the interface $\Gamma \cap T$. In other words, let

$$\widehat{\mathbf{N}}_h(T) = span\{\boldsymbol{\phi}_i^s \in (P_1(T^s))^2, s = +,- :\ \text{satisfying (3.4) below}\}. \quad (3.3)$$

$$\frac{1}{|e_j|}\int_{e_j}\phi_{i1}=\delta_{ij},\ j=1,2,3, \tag{3.4a}$$

$$\frac{1}{|e_j|}\int_{e_j}\phi_{i2}=\delta_{i-3,j},\ j=4,5,6, \tag{3.4b}$$

$$[\![\boldsymbol{\phi}_i]\!]_\Gamma=0, \tag{3.4c}$$

$$[\![2\mu\boldsymbol{\sigma}(\boldsymbol{\phi}_i,0)\cdot\mathbf{n}]\!]_\Gamma=0. \tag{3.4d}$$

We state proposition regarding the existence and uniqueness of the basis functions.

Proposition 3.1. *The function $\widehat{\boldsymbol{\phi}}$ in (3.2) is determined uniquely by conditions (3.4).*

Proof The proof can be found in [19].

Now, we define the global IFE space $\widehat{\mathbf{N}}_h$ for the velocity variable to be the set of all functions satisfying

$$\begin{cases} \boldsymbol{\phi}|_T\in\mathbf{N}_h(T) & \text{if } T \text{ is a noninterface element,}\\ \boldsymbol{\phi}|_T\in\widehat{\mathbf{N}}_h(T) & \text{if } T \text{ is an interface element,}\\ \int_e\phi_1|_{T_1}=\int_e\phi_1|_{T_2} & \text{if } e \text{ is the common edges of } T_1 \text{ and } T_2,\\ \int_e\phi_2|_{T_1}=\int_e\phi_2|_{T_2} & \text{if } e \text{ is the common edges of } T_1 \text{ and } T_2,\\ \int_e\boldsymbol{\phi}=0 & \text{if } e\in\partial T \text{ is a part of the boundary } \partial\Omega. \end{cases}$$

We also need the usual space of piecewise constant for all T for pressure:

$$M_{h,0} \quad = \quad \{p_h\in L_0^2(\Omega): p_h|_T\in P_0(T),\forall T\in\mathcal{T}_h\}.$$

However, the space $\widehat{\mathbf{N}}_h\times M_{h,0}$ cannot satisfy the interpolation property for the pressure when pressure variable is discontinuous across the interface.

Now, we describe the second type of basis functions. Given a typical interface element T, we take $\boldsymbol{\phi}^E(x,y)$ as in (3.2) and set the piecewise constant pressure as

$$p^E(x,y)=\begin{cases}p^+, & (x,y)\in T^+,\\ p^-, & (x,y)\in T^-,\end{cases} \tag{3.5}$$

and require the pair $(\boldsymbol{\phi}^E,p^E)$ satisfy the following conditions:

$$\frac{1}{|e_j|}\int_{e_j}\phi_1^E=0,\ j=1,2,3, \tag{3.6a}$$

$$\frac{1}{|e_j|}\int_{e_j}\phi_2^E=0,\ j=1,2,3, \tag{3.6b}$$

$$[\![\boldsymbol{\phi}^E]\!]_\Gamma=0, \tag{3.6c}$$

$$[\![2\mu\boldsymbol{\epsilon}(\boldsymbol{\phi}^E)\cdot\mathbf{n}]\!]_\Gamma=[\![p^E\cdot\mathbf{n}]\!]_\Gamma. \tag{3.6d}$$

This is a system of twelve equations in fourteen unknowns. We add the following equations.

$$p^+=1 \text{ on } T^+, \tag{3.7a}$$

$$p^-=0 \text{ on } T^-. \tag{3.7b}$$

The fourteen conditions (3.6) - (3.7) lead to a system of linear equations in fourteen unknowns $a_\ell^s,b_\ell^s,c_\ell^s,p^s,\ell=1,2,s=+,-$.

Proposition 3.2. *The systems (3.6) - (3.7) have a unique solution pair* $(\boldsymbol{\phi}^E, p^E)$.

Proof For each $p^E = (p^+, p^-)$ satisfying (3.7a)-(3.7b)), the system of equations (3.6a)-(3.6d) is exactly the same as (3.4a-d) with modified right hand side. Hence the existence proof is the same.

Changing the role of p^+ and p^- in (3.7a,b), we obtain another enriched pair of functions for the interface element T. If $p^+ = 1$ on T^+ and $p^- = 0$ on T^- in (3.7), we denote the pair as $(\boldsymbol{\phi}_T^{E^+}, p_T^{E^+})$. On the other hands, if $p^+ = 0$ on T^+ and $p^- = 1$ on T^-, we denote the pair as $(\boldsymbol{\phi}_T^{E^-}, p_T^{E^-})$. We name the set of such pairs as $E_h(T)$, i.e.,

$$E_h(T) := \text{ span}\{(\boldsymbol{\phi}_T^{E^+}, p_T^{E^+}), (\boldsymbol{\phi}_T^{E^-}, p_T^{E^-})\}.$$

By combining $\widehat{\mathbf{N}}_h \times M_h$ and above bubble type pairs, we define the immersed finite element space $\boldsymbol{\Psi}_h$ for Stokes equation to be set of pairs of functions $(\boldsymbol{\phi}, \psi)$ satisfying

$$\begin{cases} (\boldsymbol{\phi}, \psi)|_T \in \mathbf{N}_h(T) \times M_h(T) & \text{if } T \text{ is a noninterface element,} \\ (\boldsymbol{\phi}, \psi)|_T \in \widehat{\mathbf{N}}_h(T) \times \{0\} \oplus E_h(T) & \text{if } T \text{ is an interface element,} \\ \int_e \phi_1|_{T_1} = \int_e \phi_1|_{T_2} & \text{if } e \text{ is the common edges of } T_1 \text{ and } T_2, \\ \int_e \phi_2|_{T_1} = \int_e \phi_2|_{T_2} & \text{if } e \text{ is the common edges of } T_1 \text{ and } T_2, \\ \int_e \boldsymbol{\phi} = 0 & \text{if } e \in \partial T \text{ is a part of the boundary } \partial\Omega, \\ \psi \in L_0^2(\Omega). \end{cases}$$

We give some remarks regarding the proposed space.

Remark 3.1. *The space* $\boldsymbol{\Psi}_h$ *is not equal to the IFE space proposed in [16]. Consider a typical interface element* T*. The pressure variable of* $\boldsymbol{\Psi}_h$ *has degrees of freedom on each subregion* T^s *(*$s = +, -$*), while the pressure variable in IFE space of [16] has one (average) degree of freedom on the whole* T*. An advantage of our scheme is that one can handle discontinuous pressure (see next section).*

We give a lemma regarding the satisfaction of Laplace-Young condition.

Lemma 3.3. *For any pair of functions* $(\boldsymbol{\phi}, \psi)$ *in* $\boldsymbol{\Psi}_h$*, we have* $[\![\boldsymbol{\sigma}(\boldsymbol{\phi}, \psi) \cdot \mathbf{n}]\!]_\Gamma = 0$.

Proof It suffices to consider interface element only. Suppose $(\boldsymbol{\phi}, \psi)$ is any pair of basis functions in $\boldsymbol{\Psi}_h$ and let T be any interface element. We can decompose it as

$$(\boldsymbol{\phi}, \psi)|_T = (\mathbf{v}^0, 0) + (\mathbf{v}^E, \psi),$$

where $\mathbf{v}^0 \in \widehat{\mathbf{N}}_h^0(T)$ and $\mathbf{v}^E$ is velocity part of pairs $E_h(T)$, i.e., $(\mathbf{v}^E, \psi) \in E_h(T)$. Then

$$[\![\boldsymbol{\sigma}(\boldsymbol{\phi}, \psi) \cdot \mathbf{n}]\!]_{T\cap\Gamma} = [\![\boldsymbol{\sigma}(\mathbf{v}^0, 0) \cdot \mathbf{n}]\!]_{T\cap\Gamma} + [\![\boldsymbol{\sigma}(\mathbf{v}^E, \psi) \cdot \mathbf{n}]\!]_{T\cap\Gamma} = 0,$$

by the definitions of the space $\widehat{\mathbf{N}}_h^0$ and E_h. This completes the proof.

The associated variational form

We define the associated variational form for the problem (2.1). For this purpose, we let $\mathbf{H}_h(\Omega) := (H_0^1(\Omega))^2$ + (velocity part of $\boldsymbol{\Psi}_h$). We define two bilinear forms

$$a_h(\mathbf{u}, \mathbf{v}) := \sum_{T\in\mathcal{T}_h} \left(\int_{T\cap\Omega^-} 2\mu\boldsymbol{\epsilon}(\mathbf{u}) : \boldsymbol{\epsilon}(\mathbf{v})\, \mathrm{d}x + \int_{T\cap\Omega^+} 2\mu\boldsymbol{\epsilon}(\mathbf{u}) : \boldsymbol{\epsilon}(\mathbf{v})\, \mathrm{d}x \right) + \sum_{e\in\mathcal{E}_h^N} \frac{\gamma}{|e|} \int_e [\![\mathbf{u}]\!]_e [\![\mathbf{v}]\!]_e \, \mathrm{d}s, \tag{3.8}$$

$$b_h(\mathbf{u}, \psi) := -\sum_{T\in\mathcal{T}_h} \left(\int_{T\cap\Omega^-} \psi \mathrm{div}\mathbf{u}\, \mathrm{d}x + \int_{T\cap\Omega^+} \psi \mathrm{div}\mathbf{u}\, \mathrm{d}x \right), \tag{3.9}$$

where $\mathbf{u}, \mathbf{v} \in \mathbf{H}_h(\Omega)$ and $\psi \in L^2(\Omega)$. Here, $[\![\cdot]\!]_e$ denotes the jump along the edge e and γ is some positive parameter. We remark that we need stability terms in $a_h(\cdot,\cdot)$ to ensure a coercivity property as in [19].

Finally, we propose IFEM scheme for Stokes problem: Find $(\mathbf{u}_h, p_h)$ in $\mathbf{\Psi}_h$ such that

$$\begin{aligned} a_h(\mathbf{u}_h, \mathbf{v}_h) - b_h(\mathbf{v}_h, p_h) &= (\mathbf{f}, \mathbf{v}_h), \\ b_h(\mathbf{u}_h, q_h) &= 0, \end{aligned}$$

for all $(\mathbf{v}_h, q_h)$ in $\mathbf{\Psi}_h$.

4. Numerical results

In this section, we present numerical examples. The errors in L^2 and H^1 norms for the velocity and pressure variables are reported on a rectangular domain. The numerical simulations are carried out on uniform triangulation $\mathcal{T}_h$ by right triangles having size $h = h_0 \cdot 2^{-k}$ $(k = 1, 2, ...)$ for some h_0. We define the interface as the zero set of some level function $L(x, y)$ which is used to separate subdomains, i.e., $\Omega^- = \{(x, y) \in \Omega \,|\, L(x, y) < 0\}$ and $\Omega^+ = \{(x, y) \in \Omega \,|\, L(x, y) > 0\}$. We consider three problems. In first two examples, some known exact solutions are given to satisfy the Laplace-Young condition. In particular, we consider the case of discontinuous pressure variable in Example 4.1. In the third example, we consider a *driven cavity* benchmark problem.

In all the examples, we choose penalty parameter $\gamma = 20\mu$ in (3.8). In Example 4.1 and Example 4.2 we observe the optimal orders of error.

Example 4.1. *In this example, the interface is given by zero sets of* $L(x, y) = x + y - r = 0$ *with* $r = -0.1$. *The parameters are* $\mu^- = 10$ *and* $\mu^+ = 0.1$. *Exact solutions are*

$$\mathbf{u} = \begin{cases} \left((x+y-r)e^{(x+y-r)^2} + y^2, -(x+y-r)e^{(x+y-r)^2} + x^2\right)^T & \text{on } \Omega^+, \\ \left(\frac{\mu^+(e^{x+y-r}-1)+\mu^- y^2}{\mu^-}, \frac{\mu^- x^2 - \mu^+(e^{x+y-r}-1)}{\mu^-}\right)^T & \text{on } \Omega^-. \end{cases}$$

$$p = \begin{cases} p_0, & \text{on } \Omega^+, \\ 2(\mu^+ - \mu^-)(x+y) + p_0, & \text{on } \Omega^-, \end{cases} \qquad \text{where } p_0 = 5.220703125.$$

The errors in L^2 *and* H^1 *norms for* $\mathbf{u}_h$ *and* L^2 *error for* p_h *are reported in Table 1. We observe that both variables converge in optimal orders. The graphs of* $u_{h,1}$, $u_{h,2}$ *and* p_h *are shown in Figure 3.*

$1/h$	$\|\mathbf{u}-\mathbf{u}_h\|_0$	order	$\|\mathbf{u}-\mathbf{u}_h\|_{1,h}$	order	$\|p-p_h\|_0$	order
2^0	9.643×10^{-1}		1.691×10^{1}		1.726×10^{1}	
2^1	3.181×10^{-1}	1.600	1.111×10^{1}	0.605	5.569×10^{0}	1.632
2^2	9.137×10^{-2}	1.800	5.846×10^{0}	0.927	1.564×10^{0}	1.832
2^3	2.834×10^{-2}	1.689	3.030×10^{0}	0.948	5.559×10^{-1}	1.492
2^4	7.897×10^{-3}	1.843	1.550×10^{0}	0.967	2.615×10^{-1}	1.088
2^5	2.076×10^{-3}	1.928	7.839×10^{-1}	0.984	1.279×10^{-1}	1.031
2^6	5.317×10^{-4}	1.965	3.941×10^{-1}	0.992	6.351×10^{-2}	1.010
2^7	1.345×10^{-4}	1.983	1.976×10^{-1}	0.996	3.169×10^{-2}	1.003

Table 1: L^2 and H^1 errors for the velocity and pressure variables of Example 4.1.

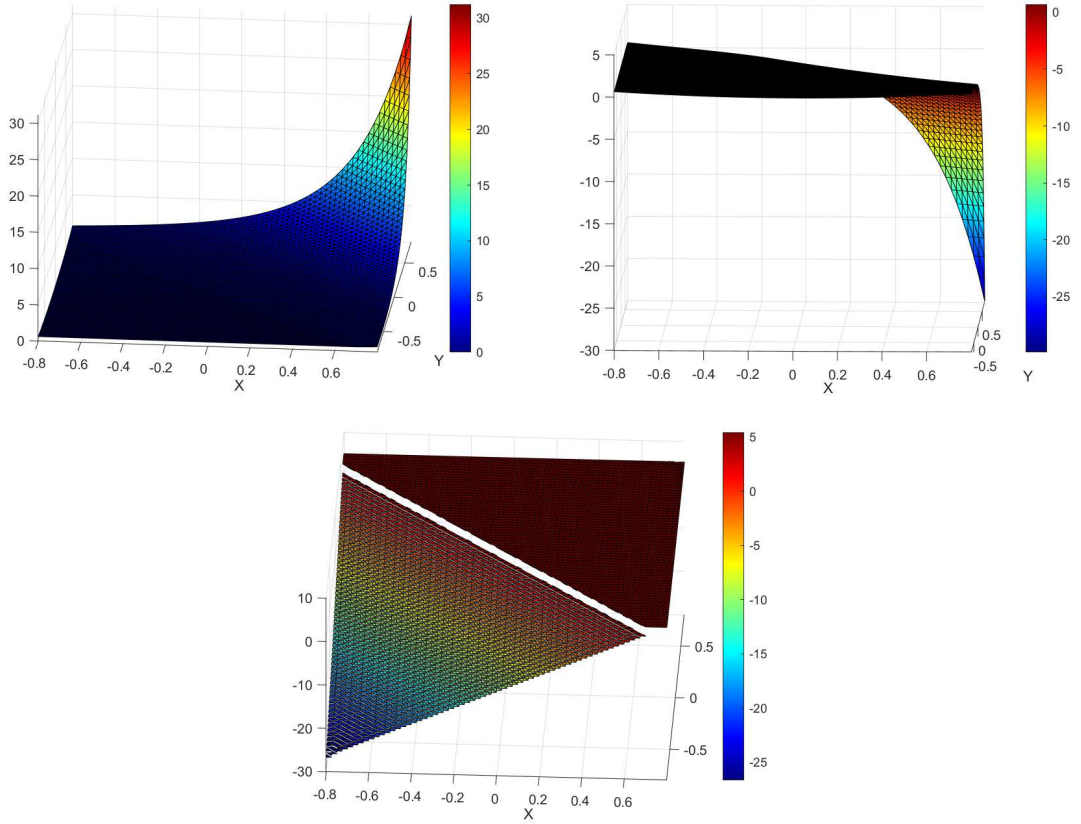

Figure 3: Plots of $u_{h,1}$ (left), $u_{h,2}$ (right) and pressure (bottom) for Example 4.1.

Example 4.2. *The interface is the zero set of* $L(x,y) = x^2 + y^2 - r^2$ *with* $r = 0.31$. *The parameters are* $\mu^- = 1$ *and* $\mu^+ = 100$. *The exact solutions are*

$$\mathbf{u} = \begin{cases} \left(\frac{1}{\mu^+} 2(x^2+y^2-r^2)y, -\frac{1}{\mu^+} 2(x^2+y^2-r^2)x\right)^T & \text{on } \Omega^+, \\ \left(\frac{1}{\mu^-} 2(x^2+y^2-r^2)y, -\frac{1}{\mu^-} 2(x^2+y^2-r^2)x\right)^T & \text{on } \Omega^-, \end{cases}$$

$$p = 100xy.$$

Errors for $\mathbf{u}_h$ *and* p_h *are reported in Table 2. We see the optimal convergence. The graphs of the vector field and the pressure variable are shown in Figure 4.*

Example 4.3 (Driven cavity). *We consider a well known driven cavity problem. Dirichlet boundary condition is imposed ;* $\mathbf{u} = [0,1]$ *on* $y = 1$ *and* $\mathbf{u} = [0,0]$ *if* $x = -1$, $x = 1$ *or* $y = -1$. *The interface is the zero set of* $L(x,y) = x^2 + y^2 - 0.4^2$ *and the parameters are* $\mu^- = 1$ *and* $\mu^+ = 100$. *Finally, we let the forcing vector* $\mathbf{f} = (0,1)^T$ *on the right hand side of (2.1a). The graphs of the vector field and the pressure variable are shown in Figure 5. We see that there is no spurious oscillation near the interface for both the velocity and pressure variable.*

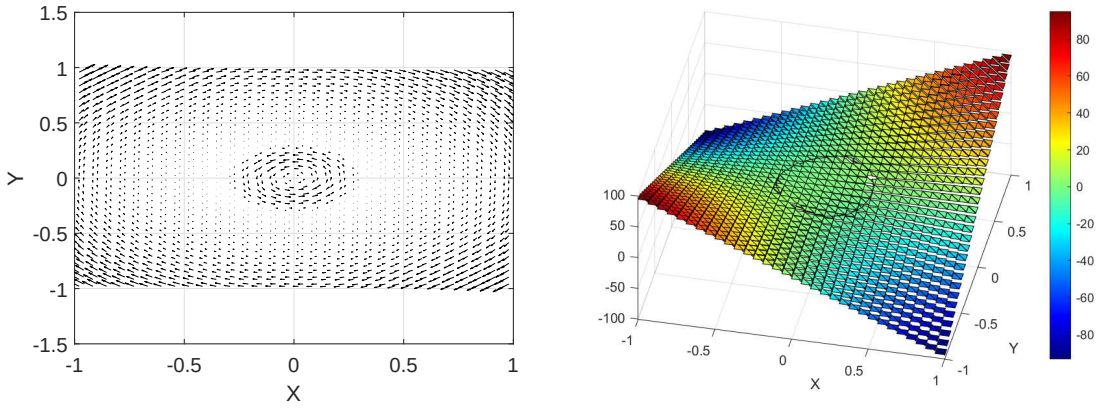

Figure 4: Plots of velocity field (left) and pressure (right) for Example 4.2.

$1/h$	$\|\mathbf{u}-\mathbf{u}_h\|_0$	order	$\|\mathbf{u}-\mathbf{u}_h\|_{1,h}$	order	$\|p-p_h\|_0$	order
2^0	2.009×10^{-1}		1.398×10^{0}		3.724×10^{1}	
2^1	1.313×10^{-2}	3.935	1.185×10^{-1}	3.560	1.983×10^{1}	0.910
2^2	8.338×10^{-3}	0.655	1.331×10^{-1}	-0.168	1.024×10^{1}	0.953
2^3	3.063×10^{-3}	1.445	6.676×10^{-2}	0.995	5.159×10^{0}	0.989
2^4	1.233×10^{-3}	1.313	4.384×10^{-2}	0.607	2.591×10^{0}	0.994
2^5	2.945×10^{-4}	2.066	1.948×10^{-2}	1.170	1.295×10^{0}	1.001
2^6	7.415×10^{-5}	1.990	8.895×10^{-3}	1.131	6.472×10^{-1}	1.000
2^7	1.844×10^{-5}	2.008	4.064×10^{-3}	1.130	3.235×10^{-1}	1.001

Table 2: L^2 and H^1 errors for the velocity and pressure variables of Example 4.2.

5. Conclusion and future work

In this work, we have developed a new IFEM for Stokes interface problems by modifying Crouzeix Raviart element. We introduce two kinds of basis functions in such a way that the coupling between the velocity and pressure variable is different. First basis functions are constructed under the assumption of the continuity of the pressure variable. In the second kind, a bubble type velocity variable is coupled with the discontinuous pressure variable. In each case, basis functions satisfy the Laplace-Young condition. Also, the pressure variable has two degrees of freedom on each interface element. Therefore, our methods can handle the discontinuous pressure case. We observe optimal convergence rates for all numerical examples.

Declaration of interests

The authors declare that they have no known competing financial interests or personal relationships that could have appeared to influence the work reported in this paper.

Acknowledgements

First author is supported by the National Research Foundation of Korea (NRF) grant funded by the Korea government (MSIT) (No. 2020R1C1C1A01005396). Second author is supported by NRF funded by MSIT (No. 2021R1A2C1003340).

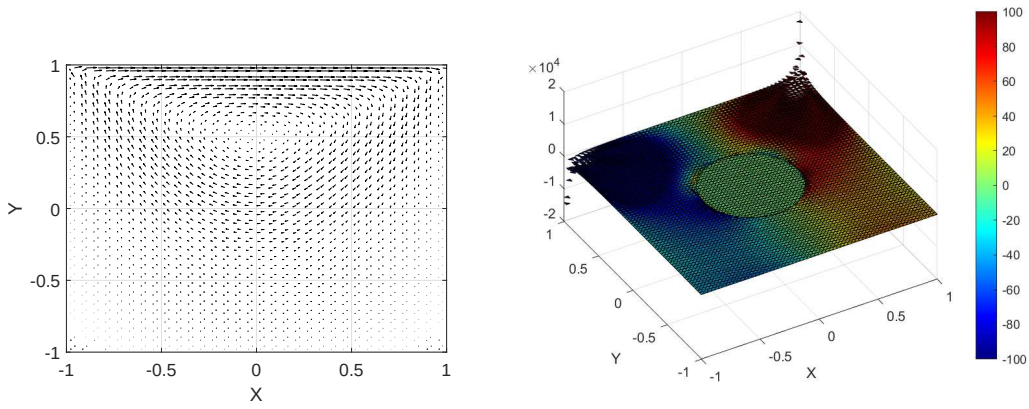

Figure 5: Graphs of the velocity field (left) and the pressure variable (right) for Example 4.3.

[1] S. Adjerid, N. Chaabane, T. Lin, An immersed discontinuous finite element method for Stokes interface problems, Comput. Methods Appl. Mech. Engrg. 293 (15) (2015) 170–190,

[2] S. Adjerid, N. Chaabane, T. Lin, P. Yue, An immersed discontinuous finite element method for the Stokes problem with a moving interface, Journal of Computational and Applied Mathematics 362 (15) (2019) 540-559.

[3] R. Becker, E. Burman, and P. Hansbo, A Nitsche extended finite element method for incompressible elasticity with discontinuous modulus of elasticity, Comput. Methods Appl. Mech. Engrg. 198 (41-44) (2009) 3352–3360.

[4] T. Belytschko, T. Black, Elastic crack growth in finite elements with minimal remeshing, International journal for numerical methods in engineering 45 (5) (1999) 601–620.

[5] J. Chessa and T. Belytschko, An extended finite element method for two-phase fluids, J. Appl. Mech. 70 (1) (2003) 10–17.

[6] S. H. Chou, D. Y. Kwak and K. T. Wee, Optimal convergence analysis of an immersed interface finite element method, Adv. Comput. Math. 33 (2) (2010) 149–168.

[7] M. Crouzeix and P. A. Raviart, Conforming and nonconforming finite element methods for solving the stationary Stokes equations, RAIRO Anal. Numér. 7 (R3) (1973) 33–75.

[8] R. Ghandriz, K. Hart, and J. Li, StressExtended finite element method (XFEM) modeling of fracture in additively manufactured polymers, Additive Manufacturing 31 (2020): 100945.

[9] S. Groß, R. Arnold, An extended pressure finite element space for two-phase incompressible flows with surface tension, Journal of Computational Physics 224 (1) (2007) 40–58.

[10] S. Groß, R. Arnold, Finite element discretization error analysis of a surface tension force in two-phase incompressible flows, SIAM journal on numerical analysis 45 (4) (2007) 1679-1700.

[11] A. Hansbo and P. Hansbo, An unfitted finite element method, based on Nitsche's method, for elliptic interface problems, Comput. Methods Appl. Mech. Engrg. 191 (47-48) (2002) 5537–5552.

[12] P. Hansbo, M. G. Larson, S. Zahedi, A cut finite element method for a Stokes interface problem, Applied Numerical Mathematics 85 (2014) 90–114.

[13] G. Jo, D. Y. Kwak, Recent development of immersed fem for elliptic and elastic interface problems, Journal of the Korean Society for Industrial and Applied Mathematics 23 (2) (2019) 65–92.

[14] G. Jo, D. Y. Kwak, A reduced crouzeix–raviart immersed finite element method for elasticity problems with interfaces, Computational Methods in Applied Mathematics 20 (3) (2020) 501–516.

[15] G. Jo, D. Y. Kwak, An IMPES scheme for a two-phase flow in heterogeneous porous media using a structured grid, Comput. Methods Appl. Mech. Engrg. 317 (2017) 684–701.

[16] D. Jones, X. Zhang, A class of nonconforming immersed finite element methods for Stokes interface problems, Journal of Computational and Applied Mathematics 392 (15) (2021): 113493.

[17] R. Kafafy, T. Lin, Y. Lin, and J. Wang, Threedimensional immersed finite element methods for electric field simulation in composite materials, International journal for numerical methods in engineering, 64 (7) (2005) 940–972.

[18] D. Y. Kwak, K. T. Wee, K. S. Chang, An analysis of a broken P_1 -nonconforming finite element method for interface problems, SIAM J. Numer. Anal. 48 (6) (2010) 2117–2134.

[19] D.Y. Kwak, S. Jin, D. H. Kyeong, A stabilized P_1-nonconforming immersed finite element method for the interface elasticity problems, ESAIM: Mathematical Modeling and Numerical Analysis, 51 (1) (2017) 187–207.

[20] I. Kwon, D. Y. Kwak, and G. Jo, Discontinuous bubble immersed finite element method for Poisson-Boltzmann-Nernst-Planck model, Journal of Computational Physics, 438 (2021): 110370.

[21] G. Legrain, N. Moes, and E. Verron, Stress analysis around crack tips in finite strain problems using the extended finite element method, International Journal for Numerical Methods in Engineering, 63 (2) (2005) 290–314.

[22] Z. Li, T. Lin, and X. Wu, New cartesian grid methods for interface problems using the finite element formulation, Numerische Mathematik, 96 (1) (2003) 61–98.

[23] Z. Li, T. Lin, Y. Lin, and R. C. Rogers, An immersed finite element space and its approximation capability, Numerical Methods for Partial Differential Equations, 20 (3) (2004) 338–367.

[24] T. Lin, and J. Wang, The immersed finite element method for plasma particle simulation, 41 st AIAA Aerospace Sciences Meeting and Exhibit (2003).

[25] T. Lin, Y. Lin, R. C. Rogers, L. M. Ryan, A rectangular immersed finite element method for interface problems, Advances in computation. Theory Pract. 7 (2001) 107–114.

[26] N. Moës, J. Dolbow, T. Belytschko, A finite element method for crack growth without remeshing, International journal for numerical methods in engineering 46 (1) (1999) 131–150.

[27] N. Moës and T. Belytschko, Extended finite element method for cohesive crack growth, Engineering fracture mechanics, 69 (7) (2002) 813–833.

[28] Arnold Reusken, Analysis of an extended pressure finite element space for two-phase incompressible flows, Computing and visualization in science 11 (4) (2008) 293–305.

[29] S.-N. Roth, P. Léger, A. Soulaïmani, *Strongly coupled XFEM formulation for non-planar three-dimensional simulation of hydraulic fracturing with emphasis on concrete dams*, Comput. Methods Appl. Mech. Engrg. 363 (1) (2020): 112899.

[30] S. Vallaghé, T. Papadopoulo, A trilinear immersed finite element method for solving the electroencephalography forward problem, SIAM J. Sci. Comput. 32 (4) (2010) 2379–2394.

[31] N. Wang, J. Chen, A Nonconforming Nitsches Extended Finite Element Method for Stokes Interface Problems, Journal of scientific computing 81 (1) (2019) 342–374.

[32] L. T. Zhang, M. Gay, Immersed finite element method for fluid-structure interactions, Journal of Fluids and Structures 23 (6) (2007) 839–857.